JHEP

Published for SISSA by Springer

Received: November 5, 2012
Accepted: December 11, 2012
Published: January 14, 2013

Single top and Higgs associated production as a probe of the $Ht\bar{t}$ coupling sign at the LHC

Sanjoy Biswas,[a] **Emidio Gabrielli**[b,c,1] **and Barbara Mele**[a]

[a] *INFN, Sezione di Roma,*
c/o Dipartimanto di Fisica, Università di Roma "La Sapienza",
Piazzale Aldo Moro 2, I-00185 Rome, Italy
[b] *NICPB,*
Ravala 10, Tallinn 10143, Estonia
[c] *INFN, Sezione di Trieste,*
Via Valerio 2, I-34127 Trieste, Italy

E-mail: Sanjoy.Biswas@roma1.infn.it, emidio.gabrielli@cern.ch, Barbara.Mele@roma1.infn.it

Abstract: The LHC sensitivity to an anomalous Higgs coupling to the top quark in the Higgs-top associated production is analyzed. Thanks to the strong destructive interference in the t-channel for standard model couplings, this process can be very sensitive to both the magnitude and the sign of a nonstandard top-Higgs coupling. We analyze cross sections and the main irreducible backgrounds for the $H \to \gamma\gamma$ decay channel. Sensitivities to an anomalous sign for the top Yukawa coupling are found to be large. In particular, at $\sqrt{s} = 14\,\text{TeV}$, assuming a universal rescaling in the Yukawa sector, a parton-level analysis with realistic selection cuts gives a signal-to-background ratio $S/B \sim 5$, for $-1.5 \lesssim Y_t/Y_t^{SM} \lesssim 0$. A number of events $S \simeq 10$ (with corresponding significances $\sim 3\ \sigma$) are expected for $60\,\text{fb}^{-1}$, to be compared with the standard-model expectation $S \sim 0.3$.

Keywords: Higgs Physics, Beyond Standard Model, Standard Model

ArXiv ePrint: 1211.0499

[1] On leave of absence from Dipartimento di Fisica, Università di Trieste, Strada Costiera 11, I-34151 Trieste, Italy.

doi:10.1007/JHEP01(2013)088

JHEP01(2013)088

Contents

JHEP01(2013)088

1 Introduction

After many years of challenging experimental searches, a signal consistent with a Higgs-boson has finally been consolidated at the LHC, with production rates compatible with the standard model (SM) predictions [1, 2]. We are now entering a new phase in Higgs boson physics, where (apart from looking for possible further Higgs physical states) the actual properties of this new particle will be determined by measuring its couplings to the other known particles with ever increasing precision. The Higgs couplings to heavy vector bosons were indirectly detected through electroweak precision tests even before an Higgs signal direct observation [3]. On the other hand, in order to constrain the Yukawa sector, which describes the Higgs couplings to fermions, we have to rely on the Higgs direct-observation profile. Indeed, electroweak precision tests are not yet sensitive at a measurable level to Yukawa coupling effects, which enter only at 2-loop level [4]. There is now a first direct determination of the $H \to b\bar{b}$ decay recently claimed at Tevatron [5], while the LHC will likely be sensitive at the $2\,\sigma$ level to both the $Hb\bar{b}$ and $H\tau\tau$ SM couplings with the statistics accumulated by the end of 2012 [6]. Nevertheless, by making proper theoretical assumptions, one can already constrain at the LHC the actual characteristics of the Yukawa sector of a Higgs boson [7]. For instance, by assuming a *universal* scale factor C_f for the Higgs Yukawa couplings to all fermion species f

$$Y_f = C_f \, Y_f^{SM} \,, \tag{1.1}$$

(where $Y_f^{SM} = m_f/v$ is the SM Yukawa coupling and $v = \langle H \rangle$ is the vacuum expectation value of the Higgs field) and a further scale factor describing the HVV (where $V = W, Z$) couplings

$$g_{HVV} = C_V \, g_{HVV}^{SM} \,, \tag{1.2}$$

present data already constrains the fermion Yukawa couplings Y_f to be inside two regions of values of opposite signs [8, 9]. In particular, if no new physical degrees of freedom is present, the ATLAS fit pinpoints at 95% C.L. the intervals [-1.5,-0.5] and [0.5,1.7] for the scale factor C_f , and the interval [0.7,1.4] for the W/Z scale factor C_V (where $C_{f,V}$ =1 in the SM) [10]. On the other hand, the CMS fit restricts the analysis to positive values of the Yukawa couplings, and finds C_f and C_V in the intervals [0.3, 1.0] and [0.7,1.2], respectively, at 95% C.L.[1] [11].

One should keep in mind that an opposite sign in the Yukawa couplings with respect to the SM prediction would have a dramatic impact on the EW breaking mechanism, even if its magnitude were close to 1. This is because the relative sign of the Higgs coupling to fermions and gauge vector bosons is crucial for recovering the unitarity and renormalizability of the theory [12]. Therefore, a negative sign in the Yukawa coupling would be an evidence of new physics that could manifest itself in many different ways. Starting from the appearance of new Higgs bosons or weakly interacting resonances in the spectrum, in case one wants to recover perturbative unitarity, up to a new strongly interacting regime of weak gauge bosons with fermions above the TeV scale. Furthermore, flipping the sign of the ttH coupling may lead to catastrophic vacuum instabilities [13].

The only fermion species that sensibly contribute to the above LHC fits are the top quark (that enters in the loop of the main Higgs production mechanism $gg \to H$, and contributes with maximal weight to the fits), the b quark and the τ lepton, under the hypothesis $C_t = C_b = C_\tau$.

The two non-degenerate opposite-sign intervals for the top-Yukawa coupling arise from the SM (destructive) interference between the W vector-boson loop and the top-quark loop in the $H \to \gamma\gamma$ amplitude. Indeed, the present moderate enhancement observed in the $H \to \gamma\gamma$ rate with respect to the SM predictions (see e.g. [14, 15], and references therein) could be related to a decreased top-Yukawa coupling, or even to a change in the relative sign of the W-Higgs and top-Higgs couplings. The latter could considerably enhance the $H \to \gamma\gamma$ branching ratio, without affecting the $gg \to H$ production rate.

A strictly fermiophobic Higgs interpretation, where C_f =0, and C_V =1, has been excluded by the LHC for the observed resonance. One should however keep in mind that, in *realistic* fermiophobic models, non-vanishing Yukawa couplings are generated at least at the radiative level by the chiral symmetry breaking induced by the non-vanishing fermion masses. Note that, in *effective* fermiophobic models, a radiatively generated top Yukawa coupling tends to have an opposite sign with respect to its SM value [4].

In this paper, we address the problem of the determination of the relative sign of the ttH and WWH couplings through the study of the Higgs production in association with a single top quark at the LHC. While the magnitude of the top and W couplings can be directly measured, respectively, through the Higgs boson production in association with a top pair (see [16] for a recent study), and in vector-boson-fusion or HW-associated production, all these processes are not affected by the top and W couplings relative sign. The

[1]Note that ATLAS and CMS obtain the 95%C.L. C_f and C_V intervals with different marginalization procedures.

JHEP01(2013)088

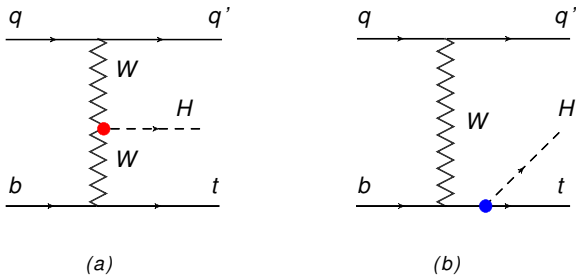

Figure 1. Feynman diagrams for the single-top plus Higgs associated production in the t-channel $q\,b \to t\,q'H$ at hadron colliders. Higgs radiation by the initial b-quark line is not shown (see text).

t-channel for single top and Higgs associated production is, on the other hand, particularly sensitive to the Y_t and g_{HWW} relative phase, because of the strong destructive interference in the SM matrix element of the two Feynman graphs for $qb \to tq'H$ in figure 1 [17].

The associated production of a Higgs and a single top quark at the LHC and the SSC (the Superconducting Super Collider) was analyzed in the SM for a light Higgs boson in [18]–[20] (with [18] focusing on the $H \to \gamma\gamma$ decay). In [21] (see also [22]), a Higgs decaying into $b\bar{b}$ pairs was studied for the same process at the LHC. However, quite negative conclusions were reached for both the $H \to \gamma\gamma$ and $H \to b\bar{b}$ modes in the SM. The extension to a minimal supersymmetric two Higgs-doublet model slightly improves the expectations. In [22], the $H \to WW^{(*)}, ZZ^{(*)}$ decays were studied for Higgs masses $150\,\text{GeV} < m_H < 200\,\text{GeV}$. Both a SM Higgs and a variable Y_t-strength setups (including the possibility of switching the g^{SM}_{HVV} sign) were considered. Good sensitivities in the above m_H range were found for a non-standard relative sign of the Higgs couplings to W and top quarks.

Among the three processes contributing to the associated production of a Higgs and a single top quark process (t-channel $q\,b \to tq'H$, s-channel $q\bar{q}' \to t\bar{b}H$, and W associated production $g\,b \to WtH$), here we concentrate on the t-channel $q\,b \to tq'H$. Indeed, as we will explicitly show, for a Higgs boson as light as 125 GeV, the latter has the largest cross section at the LHC, and the highest sensitivity to anomalous Y_t couplings coming from the interference effects of the two Feynman diagrams in figure 1 [21]. We focus on the two-photon decay $H \to \gamma\gamma$, and study the event rates for the signature corresponding to

$$q\,b \to t\,q'H \to t\,q'\gamma\gamma\,, \tag{1.3}$$

by applying realistic selection cuts based on present searches at the LHC. The rate suppression by the branching ratio (BR) for $H \to \gamma\gamma$ is then expected to be compensated by a better signal-to-background event ratio S/B. We consider the hadronic $t \to b\,qq'$ decay, and estimate the corresponding main *irreducible* backgrounds at parton level, requiring the tagging of a b jet in the final state. Present experimental studies of the $H \to \gamma\gamma$ decay suggest that the contribution of the reducible backgrounds where photons are misidentified is subdominant [23, 24]. We expect a moderate contribution also from misidentified light and b jets (see e.g. [25] as a relevant example).

We show that, while, for Y_t close to its SM value $C_t \sim 1$, the study of the $H \to \gamma\gamma$ decay channel in $p\,p \to t\,q\,H$ requires many hundreds of fb^{-1} of integrated luminosity at 14 TeV, a negative value of the top Yukawa coupling with $C_t \sim -1$ would produce a detectable signal already with a few tens of fb^{-1}. A small but detectable number of events (with excellent signal-to-background ratio S/B) are expected for $C_t \sim -1$ even at 8 TeV with the integrated luminosity available by the end of 2012.

The plan of the paper is the following. In section 2, we define the theoretical framework for the Higgs coupling dependence of the present study. In section 3, we detail the top Yukawa dependence of the single-top plus Higgs associated production cross sections for the three main production mechanisms. We define the relevant backgrounds and selection cuts for the t-channel $p\,p \to t\,q\,H$, in section 4, where we also present results on signal (S) and background (B) event numbers. In section 5, we discuss statistical significances of our results, and finally we conclude in section 6.

2 Coupling parameter setups

In the analysis of the potential of the channel $p\,p \to t\,q\,H \to t\,q\,\gamma\gamma$ at the LHC, we will focus on the dependence on both magnitude and sign of the C_t scale factor. Nevertheless, our results on the $p\,p \to t\,q\,H$ cross sections can straightforwardly be extended to a larger framework, where the W coupling factor C_W has a non-standard value. This follows from the C_W and C_t dependence of the relevant production rates for the $q\,b \to t\,q'H$ process:

$$d\,\sigma = d\,\sigma(C_W, C_t) = |C_W|^2\; d\,\sigma(1, C_t/C_W)\,. \tag{2.1}$$

Hence, the critical parameter for cross sections in the present study is the relative phase of the C_t and C_W scale factors, while a further variation in the W coupling magnitude $|C_W|$ will just affect the production rate normalization. From now on, we will then assume $C_W = C_V = 1$.

Of course, the C_V and C_f setup have an impact not only on the Higgs production cross section but also on the branching ratio

$$BR_{\gamma\gamma} \equiv BR(H \to \gamma\gamma) \tag{2.2}$$

that enters the $p\,p \to t\,q\,\gamma\gamma$ event rates. In order to make our results as model independent as possible, we will consider two different parameter setups:

- *Universal Yukawa rescaling*, that is assuming just one free parameter $C_f = C_t$ (and $C_V = 1$) both in production and decay amplitudes. $BR_{\gamma\gamma}$ is then a function of C_t, which enters both the $H \to \gamma\gamma$ width and the Higgs total width through C_f;

- *C_t and $BR_{\gamma\gamma}$ as independent parameters* (and $C_V = 1$), with C_t affecting only production cross sections, and $BR_{\gamma\gamma}$ describing the overall effect of new physics on the Higgs decay rate.

All the remaining couplings and physical degrees of freedom entering this study will be just the SM ones. The final results for the two setups can be easily related by just rescaling the event rates by the proper $BR_{\gamma\gamma}$ ratio.

JHEP01(2013)088

3 Signal production rates versus C_t

In this section, we study the $pp \to tqH$ cross section dependence on the C_t scaling factor, assuming $C_V = 1$. From now on, all the numerical cross sections discussed will refer to the hadronic pp collisions, even when the *partonic* initial state is shown. In order to compute the production rates at leading order, we used the MADGRAPH5 (v1.3.33) software package [26], with the CTEQ6L1 parton distribution functions [27]. We set both the factorization and renormalization scales at the value $Q = \frac{1}{2}(m_H + m_t)$ for the $pp \to tqH$ signal, where m_t is the top-quark mass. The other relevant parameters entering our computation are set as follow [1, 2, 28, 29]:

$$\begin{aligned} m_H &= 125\,\text{GeV}, & m_t &= 173.2\,\text{GeV}, \\ M_Z &= 91.188\,\text{GeV}, & M_W &= 80.419\,\text{GeV}, \\ m_b &= 4.7\,\text{GeV}, & \alpha_S(M_Z) &= 0.118\,. \end{aligned}$$

The SM $H \to \gamma\gamma$ branching ratio $BR^{SM}_{\gamma\gamma}$ was obtained by HDECAY [30], while the model dependent $BR_{\gamma\gamma}$ versus C_f has been evaluated via the leading-order H partial widths [31], improved by normalizing the result by a factor $BR^{SM}_{\gamma\gamma}/BR^{C_f=1}_{\gamma\gamma}$ (where $BR^{C_f=1}_{\gamma\gamma}$ is the leading-order evaluation of the SM branching ratio). For reference in the following discussion, the relevant SM cross sections σ and $BR_{\gamma\gamma}$ are (summing up cross sections over the two charge-conjugated channels)[2]

$$\sigma(q\,b \to t\,q'H)^{SM} \simeq 15.2\ \text{fb} \qquad \text{at} \quad \sqrt{s} = 8\,\text{TeV} \tag{3.1}$$

$$\sigma(q\,b \to t\,q'H)^{SM} \simeq 71.8\ \text{fb} \qquad \text{at} \quad \sqrt{s} = 14\,\text{TeV} \tag{3.2}$$

$$BR^{SM}_{\gamma\gamma} \simeq 2.29 \cdot 10^{-3} \tag{3.3}$$

In figure 2, we plot the $pp \to tqH$ production cross-section versus C_t, for $\sqrt{s} = 8\,\text{TeV}$ and $14\,\text{TeV}$. Throughout this work we focus on the range

$$-1.5 < C_t < 1.5\,, \tag{3.4}$$

where the C_t dependence is more critical, and the most favored regions of the LHC fits lie [10, 11]. Figure 2 shows that in the SM $C_t = 1$ case the destructive effect of the interference of the two diagrams in figure 1 is maximal, and that a sign change in Y_t produces a dramatic enhancement in the $pp \to tqH$ production cross sections.

Similarly, the destructive interference between the W and top loops in the $H \to \gamma\gamma$ decay gives rise to an enhancement in the width $\Gamma_{\gamma\gamma}$ after switching the C_t sign. On the other hand, the overall $BR_{\gamma\gamma}$ dependence on C_t is mostly influenced, in the $C_f = C_t$ hypothesis, by the C_f impact on the Higgs dominant decay widths into b quarks, and τ leptons.

[2]The contribution to the $pp \to tqH$ cross section of the amplitude where the Higgs is radiated by the initial b-quark line is small (at the per-mil level in the C_t range relevant here), and will be neglected in the present analysis.

JHEP01(2013)088

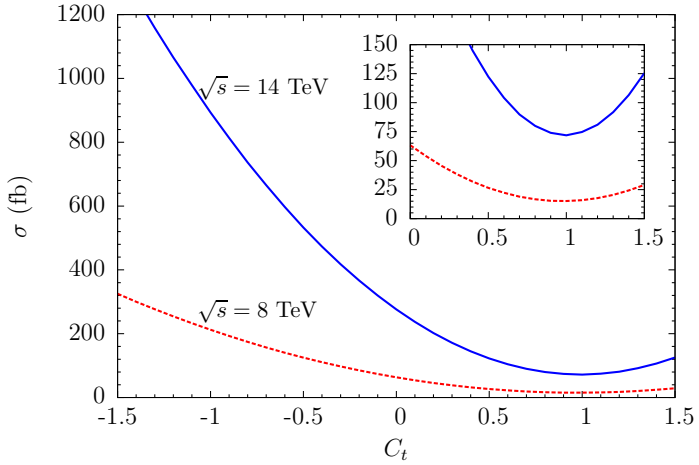

Figure 2. Production cross sections for $p\,p \to t\,q\,H$ versus C_t, for $\sqrt{s} = 8$ and 14 TeV. The inside plot is an enlargement of the positive C_t region.

Since the cross section and $BR_{\gamma\gamma}$ dependencies on C_t are both crucial for the results of the present analysis, we plot in figure 3 (for $\sqrt{s} = 8$ TeV) and figure 4 (for $\sqrt{s} = 14$ TeV) the ratios R_i of the C_t dependent $\sigma(p\,p \to t\,q\,H)$, $BR_{\gamma\gamma}$, and product $\sigma(p\,p \to t\,q\,H)\cdot BR_{\gamma\gamma}$ over the corresponding SM values, for $-1.5 < C_t < 1.5$. An enlargement of the positive C_t range is given in the lower plots of both figures. Going to negative C_f values has a dramatic effect on both cross sections and production rates for $H \to \gamma\gamma$. On the other hand, $BR_{\gamma\gamma}$ is mostly sensitive to a reduction of the $|C_f|$ magnitude, and less influenced by the C_f sign.

For the sake of completeness, we also evaluated the total cross section and C_t dependence for the top-Higgs associated production with a W in the process $g\,b \to WtH$, and for the s-channel $q\bar{q}' \to t\bar{b}H$. We obtain (summing up cross sections over the two charge-conjugated channels), at $\sqrt{s} = 14$ TeV,

$$\sigma(g\,b \to WtH)^{SM} \simeq 16.0 \text{ fb}, \tag{3.5}$$
$$\sigma(g\,b \to WtH)^{C_t=0} \simeq 34.9 \text{ fb}, \tag{3.6}$$
$$\sigma(g\,b \to WtH)^{C_t=-1} \simeq 139. \text{ fb}, \tag{3.7}$$
$$\sigma(q\,\bar{q}' \to t\,b\,H)^{SM} \simeq 2.26 \text{ fb}, \tag{3.8}$$
$$\sigma(q\,\bar{q}' \to t\,b\,H)^{C_t=0} \simeq 1.49 \text{ fb}, \tag{3.9}$$
$$\sigma(q\,\bar{q}' \to t\,b\,H)^{C_t=-1} \simeq 0.39 \text{ fb}, \tag{3.10}$$

to be compared with the t-channel cross sections, at $\sqrt{s} = 14$ TeV,

$$\sigma(q\,b \to t\,q'H)^{SM} \simeq 71.8 \text{ fb}, \tag{3.11}$$
$$\sigma(q\,b \to t\,q'H)^{C_t=0} \simeq 276. \text{ fb}, \tag{3.12}$$
$$\sigma(q\,b \to t\,q'H)^{C_t=-1} \simeq 893. \text{ fb}. \tag{3.13}$$

Although there is a nice sensitivity to C_t also in the W-associated production, we do not concentrate on this process here, because of its lower rates with respect to the t-channel $q\,b \to t\,q'H$. Nevertheless, we checked that its contribution to our event selection analysis, optimized for the $p\,p \to t\,q\,H$ process, is negligible.

JHEP01(2013)088

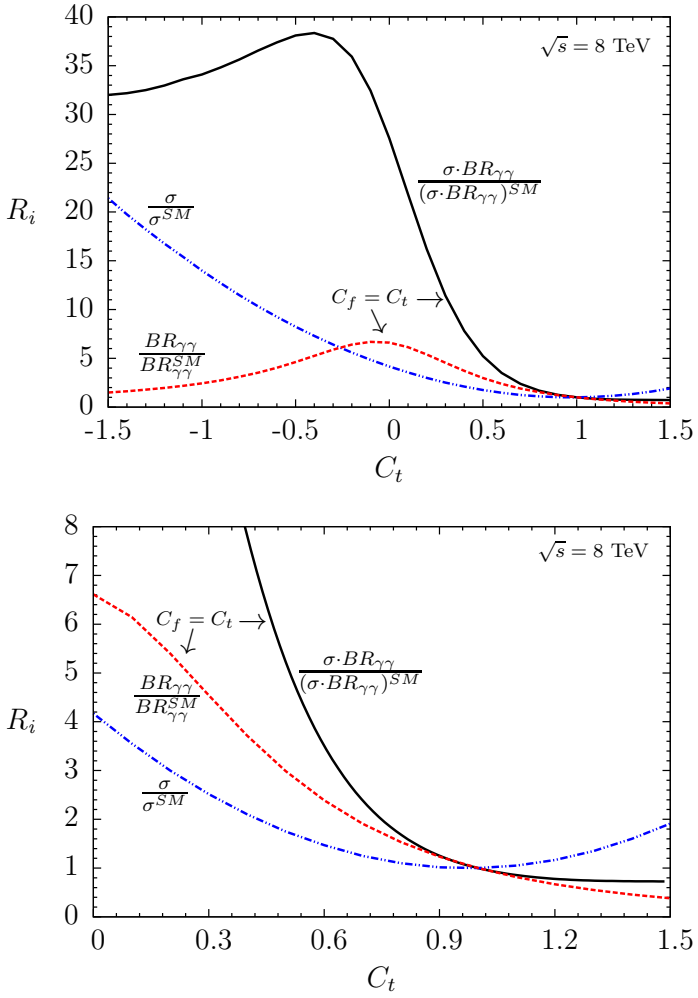

Figure 3. Enhancement factors R_i for the $p\,p \to t\,q\,H$ production cross section σ, $BR_{\gamma\gamma}$, and their product with respect to their SM values, versus C_t, for $\sqrt{s} = 8\,\text{TeV}$. The lower plot is just an enlarged view of the positive C_t range.

4 Signal versus irreducible backgrounds

The irreducible SM backgrounds for the $p\,p \to t\,q\,H \to t\,q\,\gamma\gamma$ process, for the top hadronic decay $t \to b\,q\,q'$, correspond to final states containing two photons, one b jet, and at least three light jets, i.e., $2\,\gamma + b + (\geq\ 3\,j)$. The main partonic channels contributing are top production (either single or in pair) and multi-jet final states, when accompanied by two high-p_T photons,

$$pp \to 2\,\gamma + t + j\,, \tag{4.1}$$

$$pp \to 2\,\gamma + \bar{t}\,t\,, \tag{4.2}$$

$$pp \to 2\,\gamma + b + 3\,j\,, \tag{4.3}$$

with subsequent decay $t \to b\,q\,q'$. We always require the b-jet identification in the final state.

JHEP01(2013)088

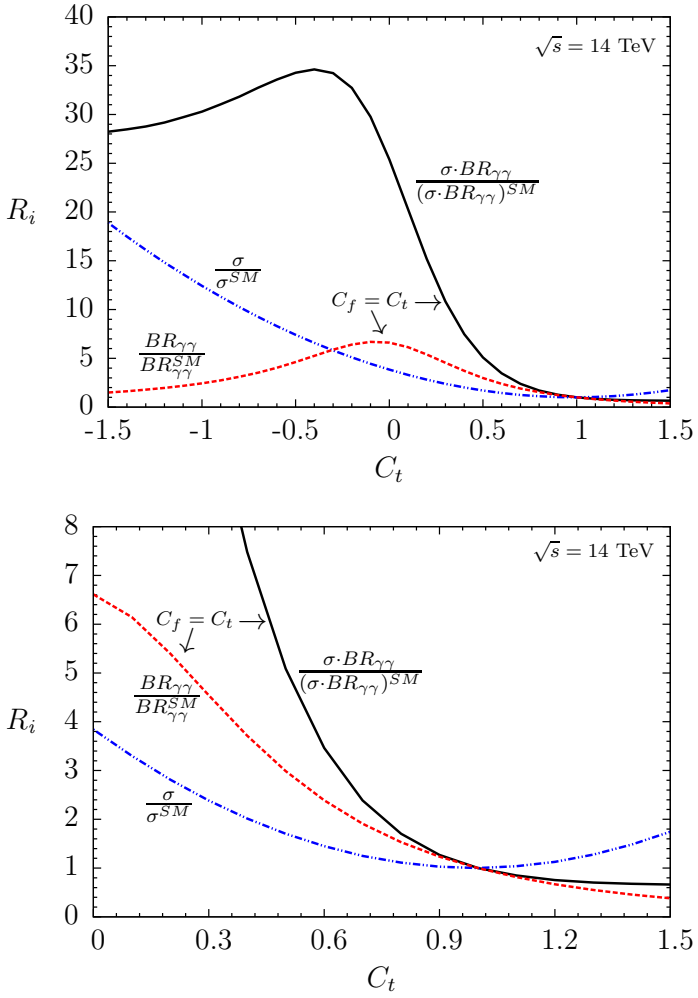

Figure 4. Enhancement factors R_i for the $p\,p \to t\,q\,H$ production cross section σ, $BR_{\gamma\gamma}$, and their product with respect to their SM values, versus C_t, for $\sqrt{s} = 14\,\text{TeV}$. The lower plot is just an enlarged view of the positive C_t range.

To study the above channels we have used the same simulation package and parton distribution functions described in section 3 with the renormalization and factorization scale set at the default dynamical scale value in MADGRAPH5 [26].

As discussed in section 1, we postpone the study of the channels contributing to the *reducible* background through misidentified particles to a more in-depth analysis, being confident that the bulk of the final background will originate from the irreducible one. In our analysis, jets are defined at the parton level.

In order to tag an event, we require the final particles to pass the following selection criteria, modeled according to present searches [23, 24]:

$$p_T^{\gamma_1} > 40\,\text{GeV}, \quad p_T^{\gamma_2} > 30\,\text{GeV}, \quad p_T^{j,b} > 25\,\text{GeV}, \quad |\eta_{\gamma,b}| < 2.5, \quad |\eta_j| < 4.5. \tag{4.4}$$

From now on, b stands for a b jet. We assume a b-tagging efficiency of 60%, which should guarantee a very good light-jet rejection factor [32]. The isolation requirement between

JHEP01(2013)088

$\sqrt{s} = 8\,\text{TeV}$ $(60\,\text{fb}^{-1})$	*Signal (S)*			*Background (B)*			
Cut	$C_t = -1$	$C_t = 0$	$C_t = 1$	$2\gamma + t + j$	$2\gamma + t\bar{t}$	$2\gamma + b + 3j$	B_{tot}
$2\gamma + b + (\geq 3\,\text{j})$	7.7	6.1	0.21	9.8	11	299	320
$\lvert\eta_j^F\rvert > 2.5$ & $p_T^F > 30\,\text{GeV}$	3.7	3.0	0.09	4.0	0.46	26	31
$\lvert M_{bjj} - m_t\rvert < 20\,\text{GeV}$	3.6	2.9	0.09	4.0	0.29	6.5	11
$\lvert M_{jj(top)} - M_W\rvert < 15\,\text{GeV}$	3.4	2.8	0.08	3.8	0.23	2.1	6.1
$\lvert M_{\gamma\gamma} - m_H\rvert < 3\,\text{GeV}$	3.4	2.8	0.08	0.14	0.02	0.68	0.84

Table 1. Number of events passing sequential cuts for the signal $p\,p \to t\,q\,H \to t\,q\,\gamma\gamma$ and irreducible SM backgrounds at $\sqrt{s} = 8\,\text{TeV}$, and integrated luminosity of $60\,\text{fb}^{-1}$, assuming $C_f = C_t$.

the final state photons, light jets j, and b jets is

$$\Delta R_{i,j} = \sqrt{\Delta\eta_{i,j}^2 + \Delta\phi_{i,j}^2} > 0.4\,, \tag{4.5}$$

with i and j running over all the final photons and jets (including b jets), $\Delta\eta$ is the rapidity gap, and $\Delta\phi$ is the azimuthal angle gap between the particle pair. Because the $p\,p \to t\,q\,H$ signal comes from a t-channel W exchange process, the light jet in the final state has normally large rapidity and high transverse momentum. In the chain of subsequent cuts applied, we therefore first require a forward jet (defined as the highest rapidity light-jet in the final state) with $|\eta| > 2.5$ and $p_T > 30$ (50) GeV at $\sqrt{s} = 8\,\text{TeV}$ (14 TeV) [22, 33]. Then, we require a top quark fully reconstructed in the hadronic mode, i.e., the invariant mass of 3-jets (out of which one is a b jet) must peak at the top mass within a mass window of 20 GeV. Then, the invariant mass of the two light jets, contributing to the top quark invariant mass, must peak at the W mass within a mass window of 15 GeV. Finally, we impose that the invariant mass of the di-photon system reconstructs the Higgs mass centered at 125 GeV within a mass window of ± 3 GeV. This set of selection cuts is quite conservative, and consistent with the present experimental analyses at the LHC. The results of the above selection procedure are shown in table 1 (for $\sqrt{s} = 8\,\text{TeV}$, and integrated luminosity of $60\,\text{fb}^{-1}$) and table 2 (for $\sqrt{s} = 14\,\text{TeV}$, and integrated luminosity of $600\,\text{fb}^{-1}$) . At $\sqrt{s} = 8\,\text{TeV}$, $60\,\text{fb}^{-1}$ could correspond to the maximal integrated luminosity expected by collecting both the ATLAS and CMS data by the end of 2012.

The numbers of events passing the sequential cuts defined above are reported for the $p\,p \to t\,q\,H \to t\,q\,\gamma\gamma$ signal, for different ($C_t = \pm 1, 0$) values (assuming $C_f = C_t$ in $BR_{\gamma\gamma}$), and main irreducible backgrounds. The first row refers to the total number of events passing the photon- and jet-tagging definition in eqs. (4.4) and (4.5), while the last column shows the total number of background events B_{tot}. One can see the efficiency of the different cuts applied to enhance the signal-to-background ratio. The signal rate is only affected by the forward-jet tag, with a corresponding reduction of a factor about 2, and passes almost unaltered the remaining cuts (the small reduction in the event numbers arising from the light-jets originating from the t decay being tagged as forward jets). The largest contribution to the background comes from the $2\,\gamma + b + 3\,j$ non-resonant final state,

JHEP01(2013)088

$\sqrt{s} = 14\,\text{TeV}$ $(600\,\text{fb}^{-1})$	*Signal (S)*			*Background (B)*			
Cut	$C_t = -1$	$C_t = 0$	$C_t = 1$	$2\gamma + t + j$	$2\gamma + t\bar{t}$	$2\gamma + b + 3j$	B_{tot}
$2\gamma + b + (\geq 3\,\text{j})$	311	249	8.9	407	396	12079	12881
$\lvert\eta_j^F\rvert > 2.5$ & $p_T^F > 50\,\text{GeV}$	121	99	3.5	161	19	551	731
$\lvert M_{bjj} - m_t\rvert < 20\,\text{GeV}$	118	97	3.5	161	11	136	308
$\lvert M_{jj(top)} - M_W\rvert < 15\,\text{GeV}$	112	92	3.3	154	8.3	43	205
$\lvert M_{\gamma\gamma} - m_H\rvert < 3\,\text{GeV}$	112	92	3.3	7.2	0.28	14	22

Table 2. Number of events passing sequential cuts for the signal $pp \to tqH \to tq\gamma\gamma$ and irreducible *SM* backgrounds at $\sqrt{s} = 14\,\text{TeV}$, and integrated luminosity of $600\,\text{fb}^{-1}$, assuming $C_f = C_t$.

that is considerably affected by both the forward-jet cut and the top- and Higgs-resonance requirements. The next background for importance is the single-top production $2\gamma + t + j$, while the top-pair channel $2\gamma + t\bar{t}$ contributes to B_{tot} negligibly.

5 Signal significance versus C_t

By comparing the signal- and background- event numbers passing all the selection cuts in the last row of table 1 and 2, the sensitivity of the $pp \to tqH \to tq\gamma\gamma$ process to a change of sign of Y_f gets clearly manifest. While a *SM* coupling configuration $Y_f/Y_f^{SM} \simeq 1$ provides a signal-to-background ratio $S/B \sim 10\%\,(15\%)$ at $\sqrt{s} = 8\,(14)\,\text{TeV}$, when $Y_f/Y_f^{SM} \simeq -1$ one reaches S/B as large as $\sim 4\,(5)$ at $\sqrt{s} = 8\,(14)\,\text{TeV}$. At $\sqrt{s} = 8\,\text{TeV}$, the signal event number is quite small. For $C_f \simeq -1$, one expects about $S = 3$ with $B \lesssim 1$, for $60\,\text{fb}^{-1}$.

On the other hand, at $\sqrt{s} = 14\,\text{TeV}$ with $600\,\text{fb}^{-1}$, one gets about $S \simeq 100$ with $B \simeq 20$ in all the negative Y_f range considered ($-1.5 \lesssim C_f \lesssim 0$), with corresponding statistical significances $S/\sqrt{(S+B)} \sim 10$. This is shown in table 3, where, for a set of different C_t values, we report the corresponding significances $S/\sqrt{(S+B)}$ at $\sqrt{s} = 14\,\text{TeV}$, and integrated luminosity of $600\,\text{fb}^{-1}$. For reference, we also show the number of tagged signal events according to the object definitions in eqs. (4.4) and (4.5), and the number of tagged events passing all the sequence of selection cuts. The relevant number of background events ($B = B_{\text{tot}}$) can be found in table 2. For convenience, we present in table 4, the number of signal events and significances at $\sqrt{s} = 14\,\text{TeV}$, for a reduced integrated luminosity of $60\,\text{fb}^{-1}$, that could be collected by ATLAS and CMS over about the first year of LHC running at $\sqrt{s} = 14\,\text{TeV}$. In table 5, the corresponding results are shown at $\sqrt{s} = 8\,\text{TeV}$, and integrated luminosity of $60\,\text{fb}^{-1}$, where a few signal events could be detected for negative C_t values, with statistical significances less than 2.

In table 3, one can notice that, in the *SM* ($C_f = C_t = 1$), the large integrated luminosities foreseen at the high luminosity (HL) LHC project (a few $10^3\,\text{fb}^{-1}$) are required in order to measure a $pp \to tqH \to tq\gamma\gamma$ signal.

In figures 5–7, we compare, at different $\sqrt{s}$ and integrated luminosities, the $pp \to tqH \to tq\gamma\gamma$ signal significances obtained in the Yukawa universal-rescaling hypothesis $C_f = C_t$, with the more model-independent framework of fixed values of the ratio

JHEP01(2013)088

$\sqrt{s} = 14\,\text{TeV}$ $(600\,\text{fb}^{-1})$	$C_t = -1.5$	$C_t = -1.$	$C_t = -0.5$	$C_t = 0$	$C_t = 0.5$	$C_t = 1.$	$C_t = 1.5$
$S\,[\,2\gamma + b + (\geq 3\,j)\,]_{\text{tag}}$	287	311	338	249	47	8.9	6.6
$S\,[\textit{passing cuts}]$	104	112	122	92	17	3.3	2.2
$S/\sqrt{S+B}$	9.3	9.7	10.	8.6	2.7	0.67	0.45

Table 3. Number of tagged events, and number of events passing all selection cuts for the $pp \to tqH \to tq\gamma\gamma$ signal at $\sqrt{s} = 14\,\text{TeV}$, and integrated luminosity of $600\,\text{fb}^{-1}$, versus C_t (assuming $C_f = C_t$). Statistical significances of the signal are shown, based on the background event numbers presented in table 2.

$\sqrt{s} = 14\,\text{TeV}$ $(60\,\text{fb}^{-1})$	$C_t = -1.5$	$C_t = -1.$	$C_t = -0.5$	$C_t = 0$	$C_t = 0.5$	$C_t = 1.$	$C_t = 1.5$
$S\,[\,2\gamma + b + (\geq 3\,j)\,]_{\text{tag}}$	29	31	34	25	4.7	0.89	0.66
$S\,[\textit{passing cuts}]$	10	11	12	9.2	1.7	0.33	0.22
$S/\sqrt{S+B}$	2.9	3.1	3.2	2.7	0.86	0.21	0.14

Table 4. Number of tagged events, and number of events passing all selection cuts for the $pp \to tqH \to tq\gamma\gamma$ signal at $\sqrt{s} = 14\,\text{TeV}$, and integrated luminosity of $60\,\text{fb}^{-1}$, versus C_t (assuming $C_f = C_t$). Statistical significances of the signal are shown, based on the background (rescaled) event numbers presented in table 2.

$\sqrt{s} = 8\,\text{TeV}$ $(60\,\text{fb}^{-1})$	$C_t = -1.5$	$C_t = -1.$	$C_t = -0.5$	$C_t = 0$	$C_t = 0.5$	$C_t = 1.$	$C_t = 1.5$
$S\,[\,2\gamma + b + (\geq 3\,j)\,]_{\text{tag}}$	7.4	7.7	8.7	6.1	1.1	0.21	0.16
$S\,[\textit{passing cuts}]$	3.2	3.4	3.8	2.75	0.52	0.08	0.06
$S/\sqrt{S+B}$	1.6	1.7	1.8	1.5	0.45	0.08	0.06

Table 5. Number of tagged events, and number of events passing all selection cuts for the $pp \to tqH \to tq\gamma\gamma$ signal at $\sqrt{s} = 8\,\text{TeV}$, and integrated luminosity of $60\,\text{fb}^{-1}$, versus C_t (assuming $C_f = C_t$). Statistical significances of the signal are shown, based on the background event numbers presented in table 1.

$R^{\gamma\gamma}_{BR} = BR_{\gamma\gamma}\,/BR^{SM}_{\gamma\gamma}$. In the latter case, the $BR_{\gamma\gamma}$ enhancement could arise from a new mechanism beyond the SM, that affects only $BR_{\gamma\gamma}$ without influencing the $pp \to tqH$ production cross section apart from its C_t dependence. For example, the presence of new heavy physical states could contribute to the $H \to \gamma\gamma$ width, without affecting the $pp \to tqH$ cross section. One can see that an enhancement factor $R^{\gamma\gamma}_{BR} \gtrsim 2$ is required in order to get at least $3\,\sigma$ significances for $C_t \sim -1$, at $\sqrt{s} = 14\,\text{TeV}$, and integrated luminosity of $60\,\text{fb}^{-1}$.

6 Conclusions

We have analyzed the t-channel $pp \to tqH \to tq\gamma\gamma$ potential for determining the relative sign of the ttH and WWH couplings at the LHC. As previously noted, the $pp \to tqH$ production cross section is extremely sensitive to a sign switch with respect to the SM. On the other hand, the actual potential of the single-top plus Higgs associated production depends on the additional theoretical assumptions on $BR_{\gamma\gamma}$. We have made

JHEP01(2013)088

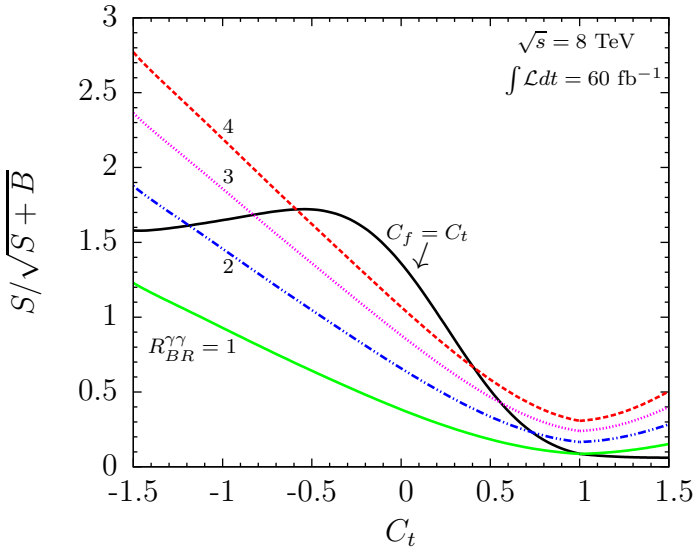

Figure 5. Signal significance versus C_t. Different assumptions are made for the value of $R^{\gamma\gamma}_{BR} = BR_{\gamma\gamma}\ /BR^{SM}_{\gamma\gamma}$. The black solid line represents the Yukawa universal-rescaling hypothesis, where $R^{\gamma\gamma}_{BR}$ is just a function of C_t, with $C_b = C_\tau = C_t$. The remaining (colored) lines refer to the constant $R^{\gamma\gamma}_{BR} = 1, 2, 3, 4$ hypothesis.

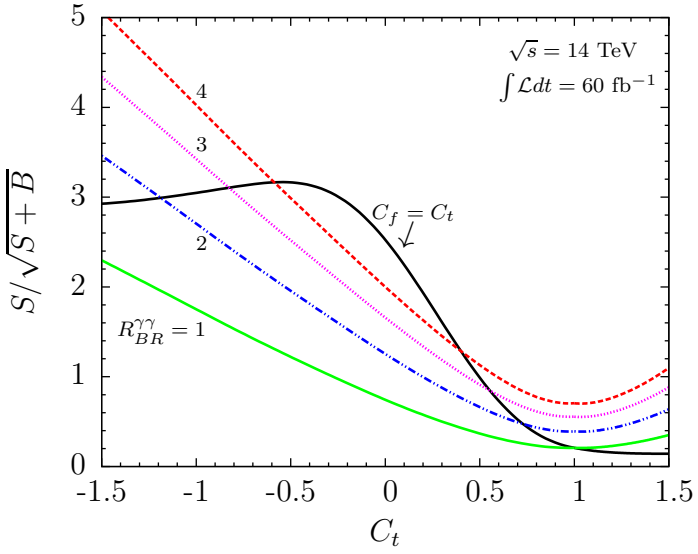

Figure 6. Signal significance versus C_t. Different assumptions are made for the value of $R^{\gamma\gamma}_{BR} = BR_{\gamma\gamma}\ /BR^{SM}_{\gamma\gamma}$. The black solid line represents the Yukawa universal-rescaling hypothesis, where $R^{\gamma\gamma}_{BR}$ is just a function of C_t, with $C_b = C_\tau = C_t$. The remaining (colored) lines refer to the constant $R^{\gamma\gamma}_{BR} = 1, 2, 3, 4$ hypothesis.

a parton-level simulation of the $H \to \gamma\gamma$ decay signal for the $pp \to t\,q\,H$ channel, and studied the corresponding main irreducible backgrounds with a quite conservative set of selection cuts on the kinematics of the final particles. We have found that the first year of the LHC running at 14 TeV could be sufficient, if $C_f = C_t \lesssim 0$, to have a considerable

JHEP01(2013)088

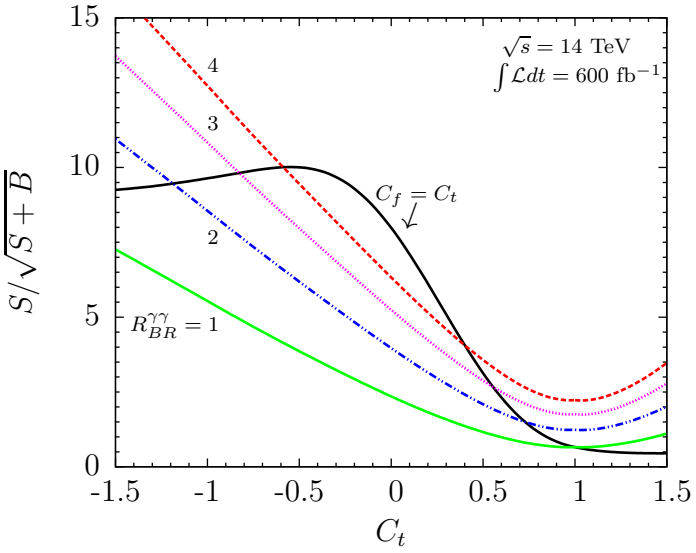

Figure 7. Signal significance versus C_t. Different assumptions are made for the value of $R^{\gamma\gamma}_{BR} = BR_{\gamma\gamma}\,/BR^{SM}_{\gamma\gamma}$. The black solid line represents the Yukawa universal-rescaling hypothesis, where $R^{\gamma\gamma}_{BR}$ is just a function of C_t, with $C_b = C_\tau = C_t$. The remaining (colored) lines refer to the constant $R^{\gamma\gamma}_{BR} = 1, 2, 3, 4$ hypothesis.

signal event number with moderate background. In particular, an integrated luminosity of $60\,\text{fb}^{-1}$ would give about 10 signal events versus less than 0.3 background events over all the negative range $-1.5 \lesssim C_t \lesssim 0$. This is to be confronted with the result corresponding to the SM parameter setup, that would require the integrated luminosities of the HL-LHC in order to reach an observable event statistics.

We then urge the LHC experimental groups to consider the single-top plus Higgs associated production $p\,p \to t\,q\,\gamma\gamma$ through a full-simulation analysis. We also leave to further work the assessment of the potential of the $p\,p \to t\,q\,H$ process as a probe of an anomalous top Yukawa behavior by means of the Higgs decays other than $H \to \gamma\gamma$.

Acknowledgments

We thank Fabio Maltoni for pointing out to us the single-top plus Higgs production sensitivity to anomalous top Yukawa couplings. Discussions with Aleksandr Azatov, Roberto Contino, Kirtiman Ghosh, Pradipta Ghosh, Satyanarayan Mukhopadhyay, and Saurabh Niyogi are thankfully acknowledged. We also thank Gennaro Corcella, Leandro Nisati, and Fulvio Piccinini for advice on event simulation, and the RECAPP, Harish-Chandra Research Institute, for providing some extra cluster computing resources. E.G. would like to thank the PH-TH division of CERN for its kind hospitality during the preparation of this work. This work was supported by the ESF grant MTT60, by the recurrent financing SF0690030s09 project and by the European Union through the European Regional Development Fund.

JHEP01(2013)088

References

[1] ATLAS collaboration, *Observation of a new particle in the search for the Standard Model Higgs boson with the ATLAS detector at the LHC*, *Phys. Lett.* **B 716** (2012) 1 [arXiv:1207.7214] [INSPIRE].

[2] CMS collaboration, *Observation of a new boson at a mass of 125 GeV with the CMS experiment at the LHC*, *Phys. Lett.* **B 716** (2012) 30 [arXiv:1207.7235] [INSPIRE].

[3] M. Baak et al., *The Electroweak Fit of the Standard Model after the Discovery of a New Boson at the LHC*, *Eur. Phys. J.* **C 72** (2012) 2205 [arXiv:1209.2716] [INSPIRE].

[4] E. Gabrielli and B. Mele, *Testing Effective Yukawa Couplings in Higgs Searches at the Tevatron and LHC*, *Phys. Rev.* **D 82** (2010) 113014 [*Erratum ibid.* **D 83** (2011) 079901] [arXiv:1005.2498] [INSPIRE].

[5] CDF and D0 collaborations, *Evidence for a particle produced in association with weak bosons and decaying to a bottom-antibottom quark pair in Higgs boson searches at the Tevatron*, *Phys. Rev. Lett.* **109** (2012) 071804 [arXiv:1207.6436] [INSPIRE].

[6] W.J. Murray, *Higgs searches (ATLAS)*, talk at the *Johns Hopkins 36th Workshop "Latest News on the Fermi scale from LHC and Dark Matter searches"*, Arcetri, Florence Italy, October 16–19 2012, http://www.ggi.fi.infn.it//index.php?p=events.inc&id=107.

[7] T. Plehn and M. Rauch, *Higgs Couplings after the Discovery*, *Europhys. Lett.* **100** (2012) 11002 [arXiv:1207.6108] [INSPIRE].

[8] A. Azatov, R. Contino and J. Galloway, *Model-Independent Bounds on a Light Higgs*, *JHEP* **04** (2012) 127 [arXiv:1202.3415] [INSPIRE].

[9] J. Espinosa, C. Grojean, M. Muhlleitner and M. Trott, *Fingerprinting Higgs Suspects at the LHC*, *JHEP* **05** (2012) 097 [arXiv:1202.3697] [INSPIRE].

[10] ATLAS collaboration, *Coupling properties of the new Higgs-like boson observed with the ATLAS detector at the LHC*, ATLAS-CONF-2012-127 (2012).

[11] CMS collaboration, *Observation of a resonance with a mass near 125 GeV in the search for the Higgs boson in pp collisions at* $\sqrt{s} = 7$ *TeV and 8 TeV*, CMS-PAS-HIG-12-020 (2012).

[12] T. Appelquist and M.S. Chanowitz, *Unitarity Bound On The Scale Of Fermion Mass Generation*, *Phys. Rev. Lett.* **59** (1987) 2405 [*Erratum ibid.* **60** (1988) 1589] [INSPIRE].

[13] M. Reece, *Vacuum Instabilities with a Wrong-Sign Higgs-Gluon-Gluon Amplitude*, arXiv:1208.1765 [INSPIRE].

[14] T. Corbett, O. Eboli, J. Gonzalez-Fraile and M. Gonzalez-Garcia, *Constraining anomalous Higgs interactions*, *Phys. Rev.* **D 86** (2012) 075013 [arXiv:1207.1344] [INSPIRE].

[15] P.P. Giardino, K. Kannike, M. Raidal and A. Strumia, *Is the resonance at 125 GeV the Higgs boson?*, *Phys. Lett.* **B 718** (2012) 469 [arXiv:1207.1347] [INSPIRE].

[16] C. Degrande, J. Gerard, C. Grojean, F. Maltoni and G. Servant, *Probing Top-Higgs Non-Standard Interactions at the LHC*, *JHEP* **07** (2012) 036 [arXiv:1205.1065] [INSPIRE].

[17] T.M. Tait and C.-P. Yuan, *Single top quark production as a window to physics beyond the standard model*, *Phys. Rev.* **D 63** (2000) 014018 [hep-ph/0007298] [INSPIRE].

[18] W.J. Stirling and D. Summers, *Production of an intermediate mass Higgs boson in association with a single top quark at LHC and SSC*, *Phys. Lett.* **B 283** (1992) 411 [INSPIRE].

JHEP01(2013)088

[19] A. Ballestrero and E. Maina, *$t\bar{b}$ H production for an intermediate mass Higgs*, *Phys. Lett.* **B 299** (1993) 312 [INSPIRE].

[20] G. Bordes and B. van Eijk, *On the associate production of a neutral intermediate mass Higgs boson with a single top quark at the LHC and SSC*, *Phys. Lett.* **B 299** (1993) 315 [INSPIRE].

[21] F. Maltoni, K. Paul, T. Stelzer and S. Willenbrock, *Associated production of Higgs and single top at hadron colliders*, *Phys. Rev.* **D 64** (2001) 094023 [hep-ph/0106293] [INSPIRE].

[22] V. Barger, M. McCaskey and G. Shaughnessy, *Single top and Higgs associated production at the LHC*, *Phys. Rev.* **D 81** (2010) 034020 [arXiv:0911.1556] [INSPIRE].

[23] Y. Chang, *Search for the scalar boson in the diphoton channel in CMS*, talk given at the *Conference Higgs Hunting 2012*, LAL, Orsay France, July 18–20 2012, http://indico2.lal.in2p3.fr/indico/conferenceDisplay.py?confId=1747.

[24] K. Peters, *Search for the scalar boson in the diphoton channel in ATLAS*, talk given at the *Conference Higgs Hunting 2012*, LAL, Orsay France, July 18–20 2012, http://indico2.lal.in2p3.fr/indico/conferenceDisplay.py?confId=1747.

[25] E. Gabrielli, F. Maltoni, B. Mele, M. Moretti, F. Piccinini, et al., *Higgs Boson Production in Association with a Photon in Vector Boson Fusion at the LHC*, *Nucl. Phys.* **B 781** (2007) 64 [hep-ph/0702119] [INSPIRE].

[26] J. Alwall, M. Herquet, F. Maltoni, O. Mattelaer and T. Stelzer, *MadGraph 5: Going Beyond*, *JHEP* **06** (2011) 128 [arXiv:1106.0522] [INSPIRE].

[27] J. Pumplin, D. Stump, J. Huston, H. Lai, P.M. Nadolsky and W. K. Tung, *New generation of parton distributions with uncertainties from global QCD analysis*, *JHEP* **07** (2002) 012 [hep-ph/0201195] [INSPIRE].

[28] CDF and D0 collaborations, *Combination of the top-quark mass measurements from the Tevatron collider*, *Phys. Rev.* **D 86** (2012) 092003 [arXiv:1207.1069] [INSPIRE].

[29] Particle Data Group collaboration, J. Beringer et al., *Review of Particle Physics (RPP)*, *Phys. Rev.* **D 86** (2012) 010001 [INSPIRE].

[30] A. Djouadi, J. Kalinowski and M. Spira, *HDECAY: a program for Higgs boson decays in the standard model and its supersymmetric extension*, *Comput. Phys. Commun.* **108** (1998) 56 [hep-ph/9704448] [INSPIRE].

[31] A. Djouadi, *The anatomy of electro-weak symmetry breaking. I: the Higgs boson in the standard model*, *Phys. Rept.* **457** (2008) 1 [hep-ph/0503172] [INSPIRE].

[32] ATLAS collaboration, *Commissioning of the ATLAS high-performance b-tagging algorithms in the 7 TeV collision data*, ATLAS-CONF-2011-102 (2011).

[33] K. Tackmann, *Search for the Higgs boson in the diphoton decay channel with the ATLAS detector*, talk at the *Conference ICHEP 2012*, Melbourne Australia, July 4–11 2012, http://indico.cern.ch/conferenceProgram.py?confId=181298.

JHEP01(2013)088